*Anal. Bioanal. Electrochem.*, Vol. 14, No. 6, 2022, 582-597

**Analytical & Bioanalytical Electrochemistry**


www.abechem.com

*Full Paper*

# An Electrochemical Strategy for the Highly Sensitive Voltammetric Determination of a Cardiovascular β-Blocking Agent in Biological Fluids

**Manjunath Megalamani,[1,a] Yuvarajgouda Patil,[1,a] Jyothi Abbar,[2] and Sharanappa Nandibewoor[1,*]**

[1]*Department of Chemistry, School of Advanced Sciences, KLE Technological University, Hubballi, Karnataka, India*

[2]*BMS Institute of Technology and Management, Bengaluru-560064, Affiliated to Visvesvaraya Technological University, Belagavi, Karnataka, India*

*Corresponding Author, Tel.: +919482173958; a: these two authors contributed equally to this paper.

E-Mail: stnandibewoor@yahoo.com

*Received: 8 March 2022 / Received in revised form: 22 June 2022 / Accepted: 22 June 2022 / Published online: 30 June 2022*

**Abstract**- In this report, different voltammetric tools such as cyclic, linear sweep, and square wave voltammetry were used to investigate acebutolol, a -blocker type of drug that is used to treat a variety of ailments, including cardiovascular disease, using a carbon paste electrode (CPE) under physiological environment. Under various phosphate buffer solutions, the voltammetric behavior of acebutolol displays two oxidation peaks and one reduction peak potentially within the range of -0.2 to 1.4 V, optimum results were obtained for pH 7.0. The electrode reaction was accompanied by two protons and two electrons transferred respectively; a probable electro-oxidation pathway has been proposed. The square wave voltammetric technique (SWV) was applied to perform a quantitative analysis of acebutolol. The linearity range was found to be between 0.06-10 µM. The LOD and LOQ were 2.06 nM and 6.88 nM, respectively which were superior to earlier methods. Furthermore, the new approach was used to determine the amounts of acebutolol in biological samples.

**Keywords-** Drug analysis; Carbon paste electrode; Acebutolol; Voltammetry; Oxidation; Urine analysis and blood plasma

## 1. INTRODUCTION

Drug monitoring plays a crucial part in pharmaceutical quality control, hence it is critical to creating inexpensive, sensitive, and efficient methods for analyzing pharmaceuticals. Acebutolol [ACB] is a cardio selective beta-blocker (atenolol, betoxolol, bisoprolol, epanolol, practolal, etc) which is used to treat angina pectoris [1], hyper tension [2] ,hypotensive circulatory diseases, hyperkinetic heart syndrome, portal hypertension, migraine, ventricular tachyarrhythmia's [3] psychosomatic illnesses or glaucoma, anxiety and hyperthyroidism [4]. Acebutolol displayed in Scheme 1 has been attributed to a number of cases of drug-induced liver impairment that have been clinically evident. Bradycardia, hypotension, tiredness, dizziness, depression, sleeplessness, memory loss, and impotence are all common adverse effects [5].

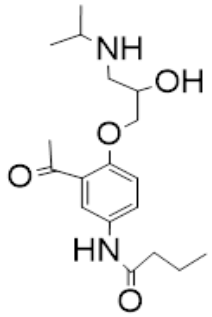


**Scheme 1.** Structure of Acebutolol

Various analytical techniques for quantifying acebutolol in biological fluids and pharmaceutical formulations are documented in literature. These analytical methods comprise of PVC membrane sensors [6], pencil graphite electrode sensor [7], gas chromatography coupled with mass spectroscopy [8], Acebutolol- tetraphenylborate-Polyvinyl chloride and Acebutolol- phosphomolybdate -Polyvinyl chloride PVC membrane sensor [9], activated screen printed carbon electrode (aSPCE) [10] ,Yttrium molybdate nanosheets modified glassy carbon electrode (YMNSs/GCE)[11], screen printed ethyl cellulose pencil graphite electrode sensor [12], molybdenum disulfide sodium alginate-polydopamine sensor(MoS2/SA-PDA) [13], exfoliated graphite titanium alloy screen printed electrode (5H-EGTA/SPCE) [14] ,spectrophotometric method [15], spectrofluorimetric method[16],analytical capillary isotachophoresis [17], capillary electrophoresis electrochemical detection [18]. However, the reported methods having technical complexity, require costly equipments, and time-consuming extraction process. To the utmost of our understanding, this is the first report on the voltammetric oxidation of ACB and evaluating of ACB in biological fluids, substantially at low-level concentrations using carbon paste electrode. The goal of this project is to make a fast, simple, and sensitive voltammetric tool for identifying ACB using a carbon paste electrode (CPE) and utilizing it to biological fluids. Voltammetric methods comprise of cyclic, linear

sweep, square wave voltammetry (SWV), and differential pulse voltammetric methodologies, among others. SWV was used frequently to study very low level determination, because it has characteristics of quick assessment, less use of electro active species, and negligible harm to the electrode surface when compared to other electro analytical techniques. On the other hand, linear sweep voltammetry (LSV) and cyclic voltammetry (CV) were also employed to determine effects of various pH, sweep rate, and other variables. In comparison to previously reported techniques, the suggested approach offers benefits such as high sensitivity, quick response, strong repeatability, and low LOD.

## 2. EXPERIMENTAL SECTION

### 2.1. Reagents and Chemicals

The chemicals were used of purely analytical in nature. Acebutolol was purchased from Sigma–Aldrich, Graphite powder extra pure was purchased from Sigma–Aldrich. The appropriate amount of ACB was dissolved in water to make the stock solution, a supporting electrolyte of phosphate buffer from pH 3.0 to 11.2 has been fabricated by mixing the appropriate proportion of $H_3PO_4$, $NaH_2PO_4$, and Na2HPO4 in Millipore water [19]. To estimate the active surface area of the working electrode Potassium ferrocyanide and potassium chloride solutions were prepared & used. The chemicals used for the preparations of phosphate buffer and estimation of surface area were purchased from molychem chemicals of analytical grade.

### 2.2. Instrumentation

The voltammetric performance of ACB was determined using CHI 6156e model electrochemical workstation, procured from United States by CH Instruments Inc. The voltammetric assays were made, to begin with connecting the workstation to the glass cell system of three-electrode, including CPE as a working electrode, a reference electrode of Ag/AgCl, and a counter electrode of a platinum wire, respectively. Against an Ag/AgCl (3 M KCl) electrode all potentials were determined. Elico LI120 pH meter (Elico Ltd, India) was employed for pH quantifications. We used a Remi R-8C Centrifuge (REMI Sales & Engineering Ltd. India) to process blood plasma samples for analysis, and the experimental temperature was reserved at 25°C± 1$^o$C.

### 2.3. Preparation of carbon paste electrode (CPE)

The CPE was developed by stirring together the graphite powder in the right amount with paraffin oil in a tiny agate mortar, then homogenizing the slurry. A fraction of the paste that resulted was firmly packed into a polytetrafluoroethylene tube's (PTFE) hallow rod. With weighing paper, the electrode's surface was smoothed. And then cleaned with water. A Copper

wire ran through the PTFE rod to the bottom of the rod connecting the paste. After each measurement, before placing a new part into the electrode, the paste was carefully discarded.

### 2.4. Area of the CPE electrode

The CV method was used to determine the electrode area. At various sweep rates, used 1.0 mM $K_4Fe(CN)_6$ as a probe. The following Randles- Sevcik **[20]** formula (1) was utilized for a reversible process:

$$I_{pa} = 0.4463\ (F^3/RT)^{1/2} n^{3/2} A_o D_o^{\ 1/2} C_o \upsilon^{1/2} \quad (1)$$

where $I_{pa}$ is the anodic peak current, n is the amount of electrons exchanged, $A_o$ is the electrodes active area of surface, $D_o$ is the diffusion coefficient, $\upsilon$ is the sweep rate, and $C_o$ is the concentrations of $K_4Fe(CN)_6$ correspondingly. The electro active surface area of CPE was determined using the slope of the $I_{pa}$ *vs.* $\upsilon^{1/2}$ plot for 1.0 mM $K_4Fe(CN)_6$ in 0.1 M KCl electrolyte, $R^2$= 8.314 J $K^{-1}$ $mol^{-1}$ , T = 298 K, F= 96,480 C $mol^{-1}$, n = 1, $D_o$=7.20 x $10^{-6}$ $cm^2$ $s^{-1}$. The electrode area in our experiment was evaluated to be 0.011 $cm^2$.

### 2.5. Analytical procedure

CPE was first activated by applying CV sweeps in the range of-0.2 to 1.4 V in a phosphate buffer solution of 0.2 M of pH 7.0 , till consecutive cyclic voltammogram was achieved. The electrodes were then transferred to other cell holding 10 ml of phosphate buffer solution having the appropriate amount of Acebutolol, and CV profiles were noted at -0.2 to 1.4 V at a scan rate of 50 $mVs^{-1}$. At a temperature of 25(±1.0) $^oC$, all measurements were taken. For varied concentrations of ACB in buffer solution the experimental condition for SWV was maintained at a sensitivity of $1\times10^{-4}$ at 0.025 Amplitude (V) and a working potential range of 0.60-1.40 V. SWV was employed for the excipient studies, urine and blood plasma samples recovery rate studies.

## 3. RESULTS AND DISCUSSION

### 3.1. Cyclic Voltammetric behavior of ACB at CPE electrode

The electrochemical behavior of ACB was examined using CV at pH 7.0 for glassy carbon electrode (GCE), gold electrode (GE), pencil graphite electrode (PGE) and CPE as working electrodes, it was found that for CPE there was enhancement of peak current and a well-defined voltammogram was observed (Figure 1, inset)., The cyclic voltammogram of 1.0 mM ACB solution at CPE acquired at a sweep rate of 50 mV/s depicts two anodic peaks, the first anodic peak (i) at 0.574 V and 15.10 µA at CPE and the second anodic peak (ii) at 1.0575 V and 80.04 µA at CPE. The outcomes are depicted in Figure 1. The reverse scan revealed only one cathodic peak (iii) at 0.082 V and 22.6 µA, showing that the electrode process is irreversible. The anodic

peak (i) was found to be reversible with the cathodic peak (iii), with a difference in potential of 1.42 V and a ratio of $I_{pa}$ to $I_{pc} \approx 0.70$. For number of sweeps at 50mV/s it was witnessed that there was a gradual decrease in the peak current indicating that oxidized product was adsorbing at the electrode surface (Figure S1). Because the anodic peak (ii) was more intense than peak (i) and was entirely irreversible, the subsequent analyses were conducted by concentrating on the more intense peak (ii) throughout the experiment.

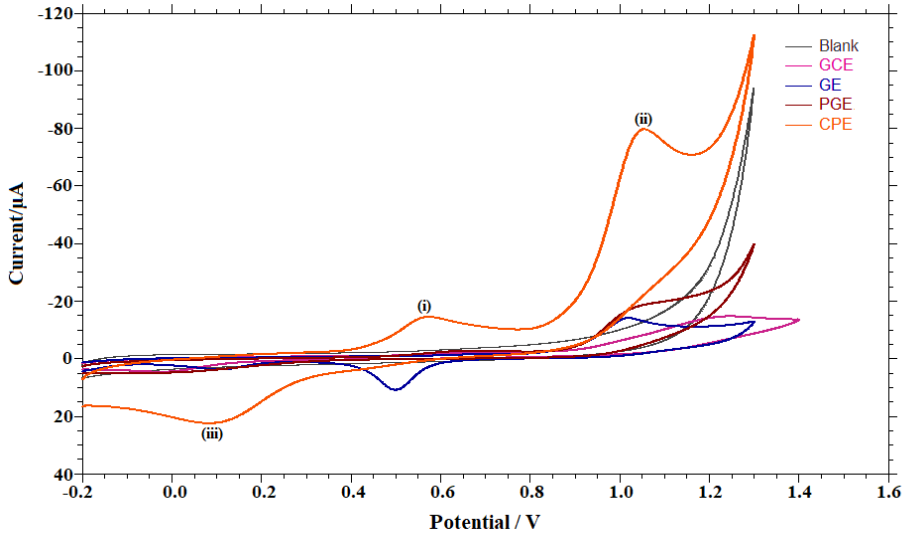


**Figure 1.** A well-defined CV profile of 1 mM ACB at 0.2 M phosphate buffer at pH 7.0 at GCE, GE, PGE and CPE. Inset: Variation in peak currents at GCE, GE, PGE and CPE.

### 3.2. Impact of pH

The CV method was used to examine the electro oxidation of 1.0mM ACB in solution of phosphate buffer over the pH of 3.0-11.2 range. Towards lesser positive values the peak potential was moved as the pH increased, and the peak current was maximum at pH 7.0, as shown in Figure 2(A), and this pH was employed throughout the experimental studies. When we plotted $E_p$ vs. pH (Figure 2(A), Inset), we got two linear zones, one in the acidic medium (pH 3.0-7.0) and the other in the basic media (pH 7.0-11.2), with slopes of -23.4mV/pH and -56.9 mV/pH, respectively. Since pH 7.0 influenced the intensity and sharpness of the peak current, the pH range of 7.0-11.2 was considered for the impact of pH on ACB, which shows the following expression:

$$E_{pa}\ (V) = -0.0569pH + 1.4681\ (R^2=0.9902) \quad (2)$$

As a result, the slope value of -56.9 mV in the pH ranges of 7.0-11.2 demonstrated that the theoretical value of -59 mV/pH was close to the actual value., signaling that the action corresponding to the second anodic peak (ii) involved an equal number of electrons and protons

(Figure 1(A)). It is obvious from the graph of $I_p$ *vs.* pH (Figure 2(B)) that the peak intensity increased and decreased in both the alkaline and acidic zones. Because pH 7 produced the best results in terms of sensitivity, as well as a stronger response it was used for further work.

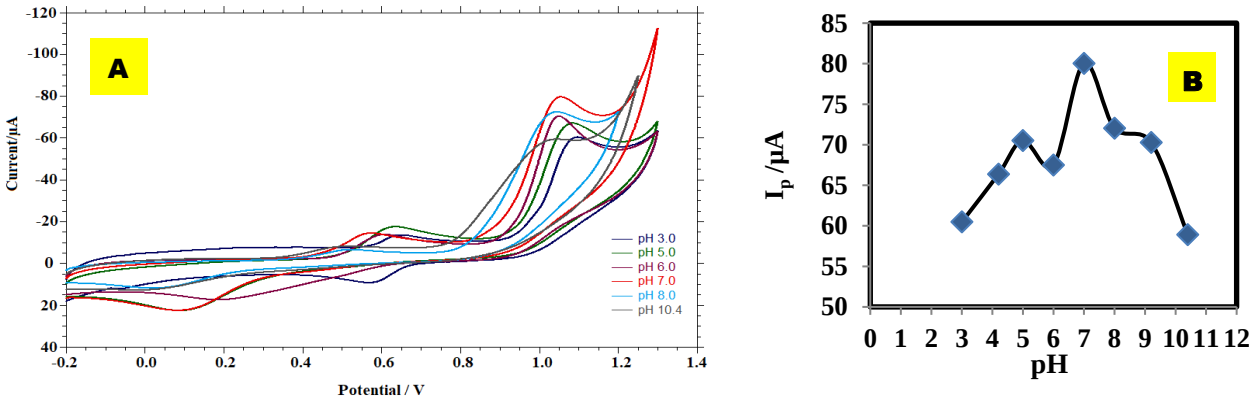


**Figure 2.** (A) CV profile of 1.0 mM ACB at CPE in solution of phosphate buffer of pH 3.0-10.4 range. Inset: Impact of pH on the peak potential of ACB at CPE, (B) Impact of pH on the peak currents of ACB

### 3.3. Impact of Sweep rate

The correlation between scan rate and peak current can provide significant facts about electrochemical systems in general. The correlation between sweep rate and peak current can also be used to define, if the reaction was electrochemically reversible or the current was regulated by mass transport or a chemical reaction involving the initial reactant. As a result to investigate the electrochemical behavior of ACB at various sweep speeds at pH 7.0 CV and LSV was utilized (Figure 3(A) and Figure 4(A)). For both Cyclic voltammetry and linear sweep voltammetry, at 0.01 to 0.40 mV/s range, linearites were produced for plot of peak current ($I_p$) against square root of sweep rate ($\upsilon$) (Fig S2 and S3). This shows that a diffusion-controlled mechanism was in charge of the operations. In the case of CV and LSV,the relevant equation (3) and (4) are given below.

$$I_p=206.78\ \upsilon\ (V/s) +6.8796,\ R^2=0.9907 \text{ for CV} \quad (3)$$

$$I_p=290.32\ \upsilon\ (V/s) +8.078,\ R^2=0.9920 \text{for LSV} \quad (4)$$

A plot of the log of the anodic peak (ii) current vs. the log of the sweep rate (Figure 3(B) and Figure 4(B)) generated a straight line with slopes of 0.40141 and 0.4027 for CV and LSV, respectively, which are close to the theoretical value of 0.5 and indicate that the electrode process is diffusion driven. The associated CV and LSV equations (5) and (6) are shown below:

$$\log I_p = 0.4027 \log \upsilon(Vs^{-1}) + 2.2873 \quad (R^2=0.9854) \quad \text{for CV} \quad (5)$$

$\log I_p = 0.4014 \log \upsilon\ (Vs^{-1}) + 2.2531$ $(R^2=0.9812)$ for LSV (6)

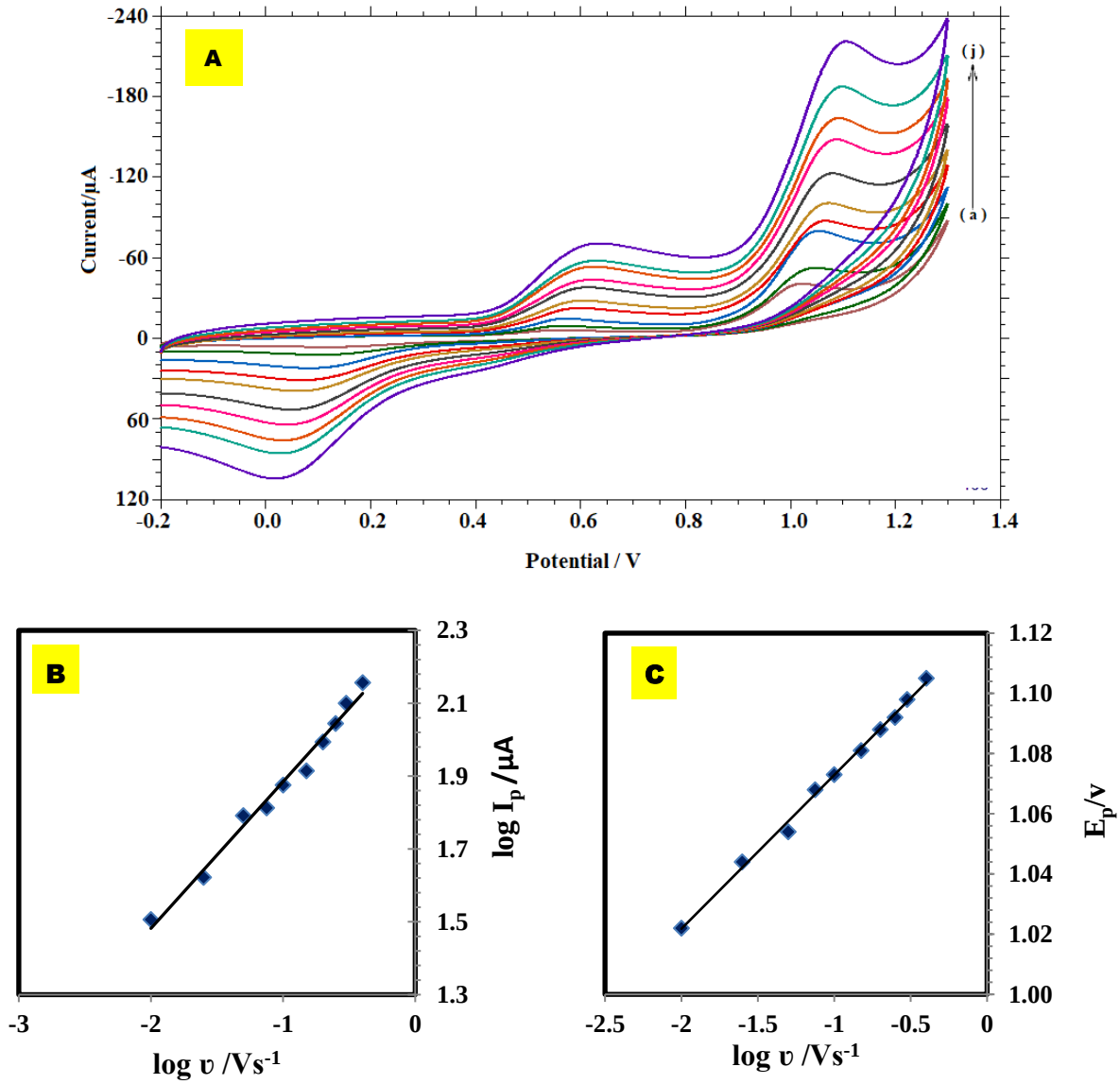


**Figure 3.** (A)CV profile of phosphate buffer of 0.2 M at pH 7.0 with ACB at different Scan rates (mV/s). (a)10 (b)25 (c)50 (d)75 (e)100 (f)150 (g)200 (h)250 (i)300 (j)400.(B) plot of log of peak current versus log of sweep rate (C) Plot of peak potential versus log of sweep rate

The oxidation peak's Ep was equally affected by the sweep rate. Once the sweep rate was increased, the peak potential switched to higher positive values, confirming that the oxidation process is irreversible. A linear association between peak potential and logarithm of sweep rate for CV and LSV (Figure 3(C) and Figure 4(C)) may be written as equations (7) and (8).

$E_p=0.0511 \log \upsilon(Vs^{-1}) + 1.124$ $(R^2=0.9963)$ for CV (7)

$E_p$=0.0521 log υ($Vs^{-1}$) + 1.1238 ($R^2$=0.9913) for LSV (8)

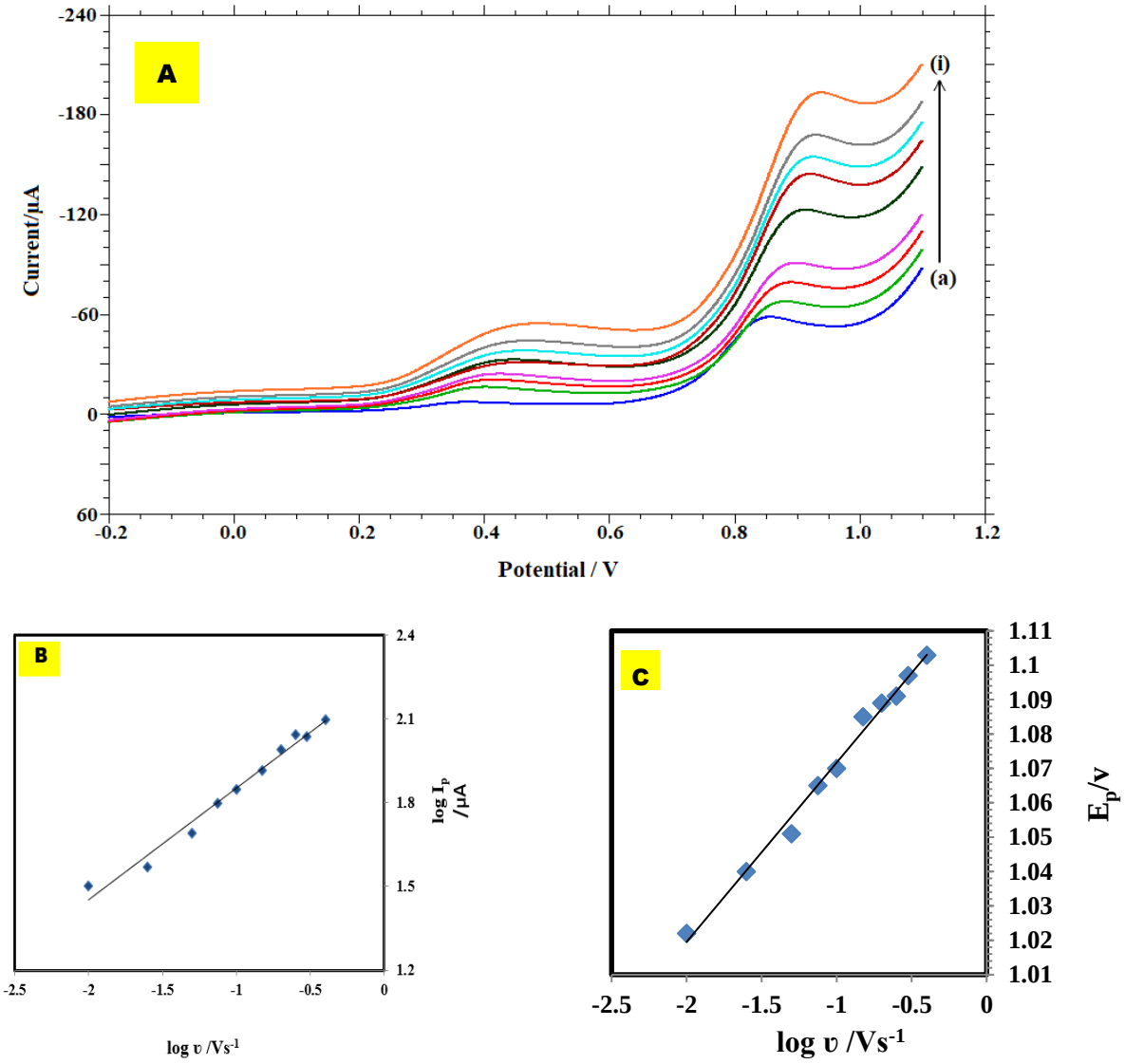


**Figure 4.** (A) LSV profile of phosphate buffer of 0.2 M at pH 7.0 with ACB at different scan rates (mV/s) . (a)25 (b)50 (c)75 (d)100 (e)175 (f)200 (g)250 (h)300 (i)400 .(B) plot of log of peak current versus log of sweep rate (C) Plot of peak potential versus log of sweep rate

According to Laviron [21], $E_p$ is well-defined by the following equation (9):

$$Ep = E°+\left(\frac{2.303RT}{\alpha nF}\right)\log\left(\frac{RTk°}{\alpha nF}\right) + \log\left(\frac{2.303RT}{\alpha nF}\right) \quad (9)$$

where α (alpha) symbolizes the transfer coefficient, $k^o$ is the reaction's typical heterogeneous rate constant, n is the number of electrons transferred, υ is the scan rate, and $E^o$ the formal redox potential. The interpretations of the other symbols are about the same as they are with the remaining portion of the symbols. As an outcome, the slope of $E_p$ vs. log υ was used to calculate

the value of n. The slope in this system is 0.0521 for CV and 0.0511 for LSV, whereas n was computed using T= 298 K and substituting the values of R and F. Agreeing to Bard and Faulkner [22, 23], α may be expressed as a mathematical equation (10):

$$\alpha = \frac{47.7}{E_{P-E_{P/2}}} \text{mV} \quad (10)$$

where $E_{p/2}$ is the potential wherein the current is half of its extreme value. As a conclusion, we calculated the value of α using both CV and LSV methodologies. The intercept of the $E_p$ vs. logυ plot (equation (7) and (8)) may be used to assess the value of $k^o$. If the value of $E^o$ in equation is derived [24] by extrapolating the vertical axis at 0 from the intercept of $E_p$ *vs.* υ. The outcomes of CV and LSV tests are shown in Table 1.

**Table 1.** Results obtained by CV and LSV from the impact of sweep rate

| Calculated Values | CV | LSV |
|---|---|---|
| **α** | 0.54 | 0.56 |
| **αn** | 1.15 | 1.13 |
| **n** | 2.11 | 2.02 |
| **$E^o$** | 1.12 | 1.13 |
| **$k^o$** | $3.4\times10^1$ $s^{-1}$ | $3.1\times10^1$ $s^{-1}$ |

### 3.4. Proposed mechanism

In the proposed approach, ACB undergoes oxidation with hydrogen loss at first, followed by hydrogen addition in the reverse reaction for the first anodic peak (i) and for the anodic peak (ii), the irreversible process includes the transfer of two electrons. As a result, for this irreversible process electrochemical mechanism was postulated, as indicated in Scheme 2. Cleavage of aromatic ether reactions have been found for the compound, according to the literature review [8]. According to this fundamental concept, the electrochemical cleavage of ACB (i) aromatic ether begins with the loss of one electron, resulting in the development of intermediate as a radical molecule, which then leads to the synthesis of two species when the water molecule is added (III and IV). On O-dealkoxylation, which is consistent with a previously described mechanism for the aromatic ether alkyl cleavage of butylated hydroxyanisole (3-tert-butyl-4-hydroxyanisole) [8]. The radical compound is formed after the second oxidation step, which involves the loss of one electron (V). Furthermore, two protons are lost resulted in the formation of N-(3-acetyl-4-oxocyclohexa-2,5-dienylidene)butyramide (VI). This observation was consistent with the previous report [7].

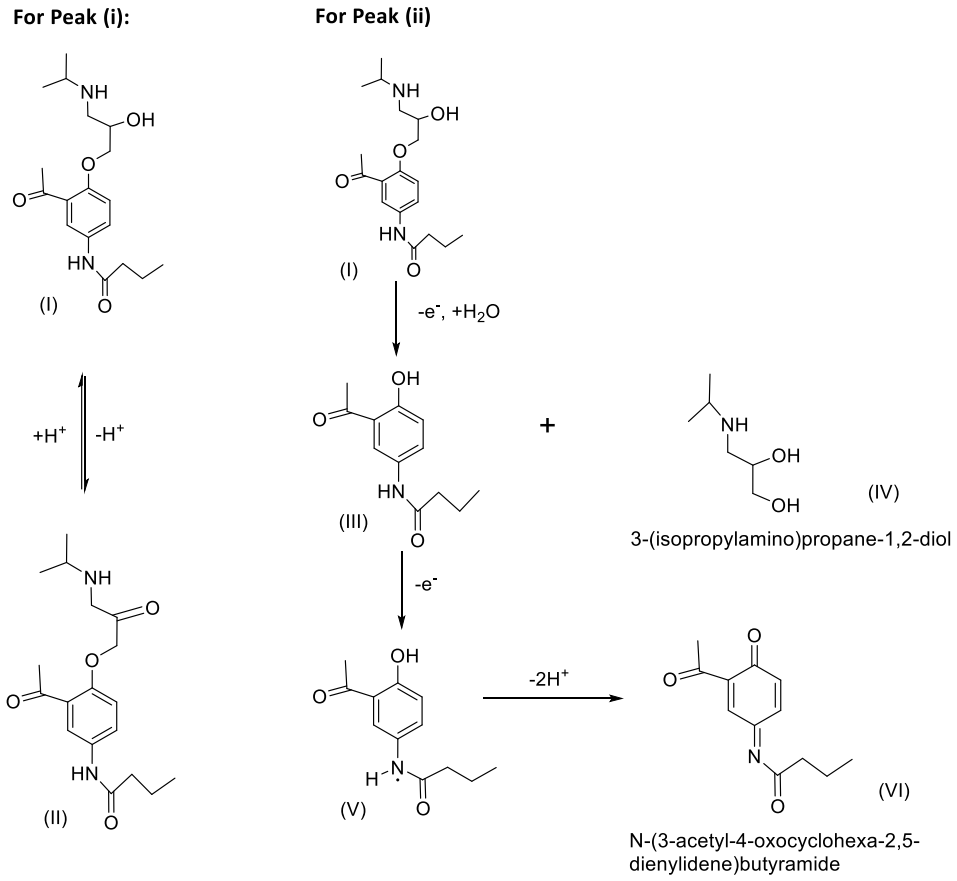


**Scheme 2.** Proposed mechanism of ACB

### 3.5. Calibration Curve and detection limit

The square wave voltammetry approach was used to determine ACB because it produced a substantially higher peak current than cyclic voltammetry. To examine the sensors sensitivity, selectivity and detection limit, a calibration curve (Figure 5) displaying the correlation of peak current on analyte concentration was developed in a broader concentration range (Figure 5, Inset).

Over the drug concentration range of 0.06 -10µM, the current vs. concentration plot (Figure 5, Inset) revealed linearity, $I_p = 0.1876[ACB] + 6.765$; $R^2=0.9917$ was the linear equation. Due to the diffusion of ACB or its oxidation products on the electrode surface, a deviation from linearity was detected for higher concentrated solutions. From the five separate calibration curves, correlated statistical data of the calibration curves were produced. The following equations were used to compute the limit of detection (LOD) and quantification (LOQ) based on the peak current:

$$LOD = \frac{3S}{m} \quad ; LOQ = \frac{10S}{m} \qquad (11)$$

where S is standard deviation of the blank's peak currents (5 trials) and m signifies the calibration curve's slope. 2.06 nM and 6.88 nM were computed as the LOD and LOQ,

accordingly. Table 2 lists the detection limits for electrochemical methods. In comparison to the existing literature, the present method's LOD and LOQ values are superior.

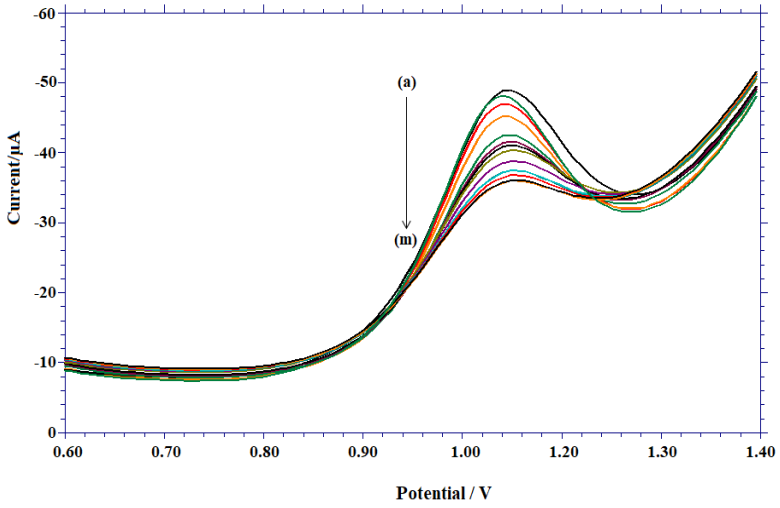


**Figure 5.** SWV of phosphate buffer of 0.2 M at pH 7.0 with ACB at various concentrations (a)120 (b)100 (c)80 (d)60 (e)40 (f)20 (g)10 (h)8.0 (i)6.0 (j)4.0 (k)2.0 (l) 1.0 (m) 0.8 at 10-7 M at CPE in 0.2 phosphate buffer solutions of pH 7.0.Inset: plot of current against concentration of ACB

The accuracy of the approach was evaluated by measuring ACB at two different concentrations over the period of intra and inter-day, with a total of three trails (n=3) falling within the linearity range. Table 3 demonstrates the precision of the techniques as a percentage of bias and RSD for intra and inter-days, suggesting that the recommended method is highly precise.

**Table 2.** ACB's linear range and detection limitations in comparison to other electrochemical methods

| Method | Linearity range (µM) | LOD (µM) | Ref |
|---|---|---|---|
| aSPCE | 0.01-200 | 0.006 | [10] |
| YMNSs/GCE | 0.01-9.6 | 0.0025 | [11] |
| ECPG/SPCE | 0.01-200 | 0.004 | [12] |
| $MoS_2$/SA-PDA | 0.009-520 | 0.005 | [13] |
| 5H-EGTA/SPCE | 0.01-15.1 | 0.003 | [14] |
| AC-TBP-PVC | 1.0-1000 | 6.0 | [9] |
| AC-PM-PVC | 1.0-1000 | 4.0 | [9] |
| PGE | 1.00-15.0 | 0.0126 | [7] |
| CPE | 0.06-10.0 | 0.00206 | Present Work |

### 3.6. Reproducibility and selectivity

A 1.0 mM ACB solution was measured in similar electrode (every time renewed) for several hours during the day to assess the electrode's stability and reproducibility; the peak current RSD was 0.285 percent (number of determinations =5). Because of CPE's remarkable stability and consistency, between-day re-reducibility was similar to within-day re-reducibility, with temperature being essentially constant (Table 3).

**Table 3**. Analytical accuracy and precision of ACB detection by SWV

| | Added ($10^{-7}$ M) | Found[a] ($10^{-7}$ M) | SD | Accuracy Bias (%) | RSD (%) |
|---|---|---|---|---|---|
| **Intra-day** | 10 | 9.99 | 0.006 | -0.09 | 0.067 |
| | 8 | 7.98 | 0.013 | -0.19 | 0.164 |
| **Inter-day** | 10 | 9.98 | 0.004 | -0.1 | 0.042 |
| | 8 | 7.98 | 0.001 | -0.13 | 0.021 |

[a]-average of five measurements

**Table 4.** Influence of excipients on the voltammetric response of 1 µM ACB

| Excipients | Concentration of Excipients/mM | $E_p$ of ACB in the absence of Excipients | $E_p$ of ACB in the presence of Excipients | Signal Change (%) |
|---|---|---|---|---|
| **$Zn^{2+}$** | 1.0 | 1.048 | 1.0365 | +1.15 |
| **$Ca^{2+}$** | 1.0 | 1.048 | 1.0166 | +3.14 |
| **$Cu^{2+}$** | 1.0 | 1.048 | 1.0261 | +2.19 |
| **$Mg^{2+}$** | 1.0 | 1.048 | 1.0387 | +0.93 |
| **Citric Acid** | 1.0 | 1.048 | 1.0156 | +3.24 |
| **D-glucose** | 1.0 | 1.048 | 1.0072 | +4.08 |
| **Lactose** | 1.0 | 1.048 | 1.0287 | +1.93 |
| **Ascorbic Acid** | 1.0 | 1.048 | 1.0386 | +0.94 |
| **Oxalic acid** | 1.0 | 1.048 | 1.0092 | +3.88 |
| **Sucrose** | 1.0 | 1.048 | 1.0492 | -0.12 |
| **Tartaric Acid** | 1.0 | 1.048 | 1.0272 | 2.08 |
| **Uric Acid** | 1.0 | 1.048 | 1.0167 | +3.13 |

### 3.7. Impact of Interferents

For the analytical application of the suggested technique, the effects of possible interferents that are expected to be identified in pharmaceutical manufacturing were examined. The tolerance limit was specified as the highest concentration of the interfering chemical that resulted in a less than 5% ACB determination error. Under ideal experimental circumstances, potential interferents effects on the voltammetric response of 1µM ACB as a standard was examined (Table 4). $Zn^{2+}$, $Ca^{2+}$, $Cu^{2+}$, $Mg^{2+}$, D-glucose, Sucrose, Lactose, Citric, Ascorbic, Oxalic, Tartaric and Uric Acids were employed at a hundredfold excess concentration, however the ACB's voltammetric signal was unaffected (Figure 6). As a result, the proposed strategy might be characterized as a one-of-a-kind technique.

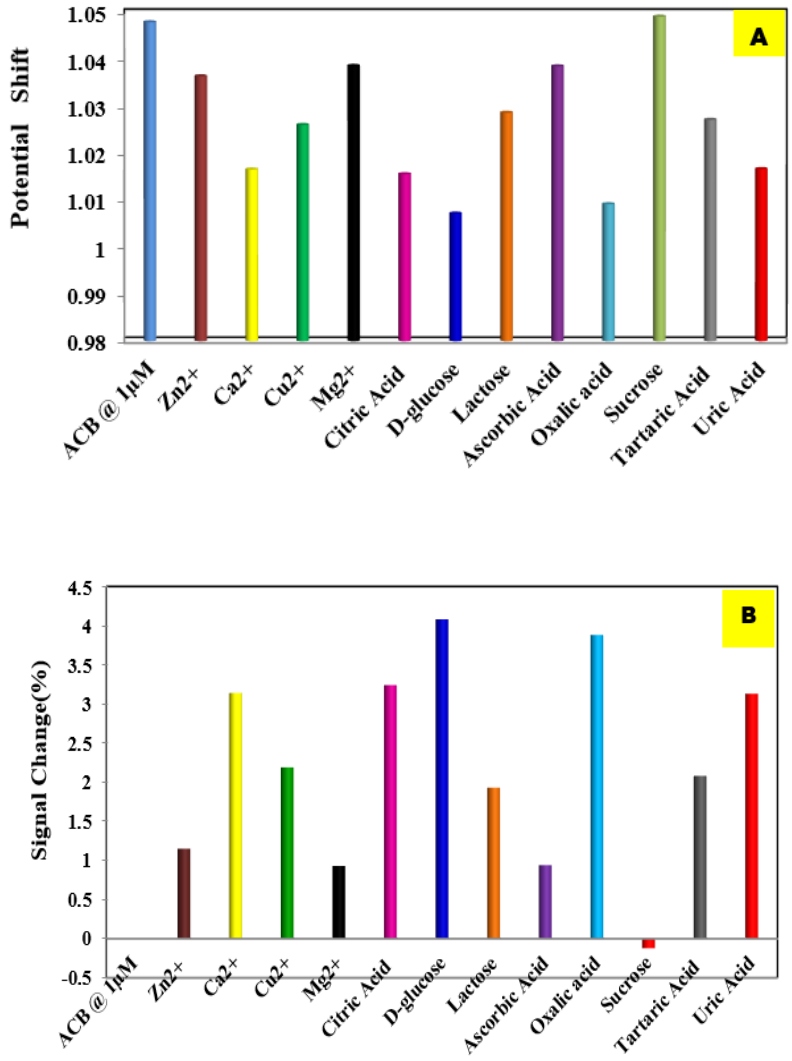


**Figure 6.** Outcome of various types of excipients on the activity of ACB (A) Potential shift of excipients (B)Signal change of excipients

### 3.8. Detection of ACB in urine samples

The suggested approach was tested for its usefulness in determining ACB in biological fluid such as human urine. Healthy participants provided drug-free urine sample, which were filtered via filter paper and kept frozen until the test. Urine samples were used to test the developed square wave voltammetric technique for determining ACB. Drug-free urine was spiked with acknowledged quantities of ACB, the recoveries from urine was assessed. Before analysis, the urine sample was diluted hundred times in pH 7.0 of 0.2 M phosphate buffer. By introducing the standard ACB solution to the system of urine sample, a quantitative analysis was performed for the investigation of spiked ACB present in the urine sample, the calibration graph was employed. Table 5 shows the detection findings of four urine samples tested. The recovery determined for urine samples was in the range of 96.7 to 101.8% with an R.S.D. of 2.35%. These matrices yielded good ACB recoveries at 95% confidence level, revealing that the suggested method's usefulness to the assessment of ACB in biological fluid could be easily assessed.

**Table 5.** The use of SWV to determine ACB levels in spiked urine samples

| Urine | Spiked ($10^{-7}$ M) | Found[a] ($10^{-7}$ M) | Recovery | SD±RSD | Margin of error | STDEV | PE | LCL | UCL |
|---|---|---|---|---|---|---|---|---|---|
| **Sample 1** | 80 | 77.42 | 96.779 | 0.00089±0.0246 | 0.0126 | 0.013 | -2.58 | -2.587 | -2.568 |
| **Sample 2** | 10 | 9.71 | 97.194 | 0.0013±0.0707 | 0.0126 | 0.013 | -0.285 | -0.297 | -0.2723 |
| **Sample 3** | 8 | 7.86 | 98.339 | 0.0027±0.1772 | 0.0167 | 0.02 | -0.132 | -0.149 | -0.1158 |
| **Sample 4** | 6 | 6.11 | 101.871 | 0.0020±0.1500 | 0.0681 | 0.07 | 0.112 | 0.016 | 0.2086 |

[a]-average of four measurements
STDEV-Std.deviation
PE-Point Estimate
LCL-Lower Confidence Limit
UCL-Upper Confidence Limit

### 3.9. Detection of ACB in blood-plasma samples

The new framework was tested for identifying ACB in biological fluid namely blood plasma. The Remi R-8C Centrifuge (REMI Sales & Engineering Ltd., India) was used to obtain blood plasma by centrifuging human blood at 3000-3500 rpm for 10-15 min, a drug-free blood plasma sample was submitted by healthy volunteer. The developed square wave voltammetric approach for identifying ACB was validated using blood plasma specimens. The recoveries from blood plasma were investigated using drug-free blood plasma spiked with known proportion of ACB. The blood plasma recoveries were evaluated. The blood plasma sample was diluted hundred times before analysis in pH 7.0 phosphate buffer. The calibration graph was used to perform a quantitative analysis for the detection of spiked ACB in blood plasma by introducing the standard ACB solution to the system of blood plasma sample. Table 6

displays the results of four blood plasma samples that were analyzed for detection. The recovery determined for blood plasma samples was in range of 97.7 to 102.6% with an R.S.D. of 2.217 %. ACB recoveries remained good in these matrices with 95% confidence level.

**Table 6**. The use of SWV to determine ACB levels in spiked blood plasma samples

| Blood-plasma | Spiked ($10^{-7}$ M) | Found[a] ($10^{-7}$ M) | Recovery | SD±RSD | Margin of error | STDEV | PE | LCL | UCL |
|---|---|---|---|---|---|---|---|---|---|
| **Sample 1** | 80 | 79.6 | 99.5033 | 0.0011±0.0305 | 0.062 | 0.637 | -0.40 | -1.024 | 0.224 |
| **sample 2** | 10 | 9.8 | 98.238 | 0.0015±0.0814 | 0.919 | 0.938 | -0.20 | -1.119 | 0.719 |
| **sample 3** | 8 | 7.82 | 97.752 | 0.0023±0.1497 | 0.381 | 0.385 | -0.19 | -0.576 | 0.197 |
| **sample 4** | 6 | 6.15 | 102.652 | 0.0014±0.1015 | 1.699 | 1.734 | 0.15 | -1.549 | 1.849 |

[a]-average of four measurements
STDEV-Std.deviation.
PE-Point Estimate.
LCL-Lower Confidence Limit.
UCL-Upper Confidence Limit.

## 4. CONCLUSION

This work investigated the voltammetric oxidation of ACB at a CPE for the first time in phosphate buffer solution under physiological conditions, i.e. pH 7.0. ACB is a diffusion-controlled two-electron–two-proton transition process. A suitable oxidation mechanism was proposed. ACB concentration and peak current was linear throughout a range as low as LOD 2.06 nM for the selected analyte. The methodology is devoid of interferents from regularly used excipients, according to a high percentage recovery and evaluation of interferents. Importantly, the results of ACB analysis in spiked urine and blood plasma specimens, verified the method's use in real-time clinical analysis. The method developed is suitable for both quality control laboratories and pharmacokinetic research requiring speed and efficiency.

### Conflict Of Interest

The authors state that they have no conflicts of interest.

## REFERENCES

[1] J. L. Rod, D. Admon, A. Kimchi, M. S. Gotsman, and B. S. Lewis, American Heart J. 98 (1979) 604.

[2] C. S. Wiysonge, H. A. Bradley, J. Volmink, B. M. Mayosi, and L. H. Opie, Cochrane Database of Systematic Rev. (2017) 1.

[3] J. G. Baker, British Journal of Pharmacology, 160 (2010) 1048.

[4] U. Borchard, J. Clinical and Basic Cardiology 1(1998) 5.

[5] B. N. Singh, W. R. Thoden, and J. Wahl, Pharmacotherapy: The Journal of Human Pharmacology and Drug Therapy 6 (1986) 45.
[6] M. R. J. Sarvestani, T. Madrakian, and A. Afkhami, J. Electroanal. Chem. 899 (2021) 115666.
[7] A. M. Bagoji, M. P. Shreekant, and S.T. Nandibewoor, Cogent Chem. (2016) 02.
[8] U. Bussy, V. Fferchaud-Roucher, I. Tea, And M. Boujtita, Electrochim. Acta 69 (2012) 351.
[9] G. A. H. Mostafa, M. M. Hefnawy, and A. Al-Majed, Sensors 7 (2007) 3272.
[10] A. Yamuna, P. Sundaresan, S. M. Chen, S. R. Sayed, T. W. Chen, S. P. Rwei, and X. Liu, Int. J. Electrochem. Sci. 14 (2019) 6168.
[11] T. W. Chen, J. V. Kumar, S. M. Chen, B. Mutharani, R. Karthik, E. R. Nagarajan, and V. Muthuraj, Chem. Engin. J. 359 (2019) 1472.
[12] A. Yamuna, P. Sundaresan, and S. M. Chen, Ultrasonics Sonochemistry 64 (2020) 105014 .
[13] C. Y. Lee, A. Prasannan, V. Lincy, S. Vetri Selvi, S. Chen, and P. D. Hong, Microchim. Acta 188 (2021) 1.
[14] N. Karikalan, M. Elavarasan, and T. C. Yang, Ultrasonics Sonochemistry 56 (2019) 297.
[15] M. M. Ayad, H. E. Abdellatef, M. M. El-Henawee, and H. M. El-Sayed, Spectrochimica Acta A 66 (2007) 106.
[16] M. A. El Dawya, M. M. Mabrouk, and R. A. El Barbary, Chemical and Pharmaceutical Bulletin 54 (2006) 1026.
[17] M. Pospíšilová, A. Kavalírová, and M. Polášek, J. Chromat. A 1081 (2005) 72.
[18] X. Li, D. Zhu, and T. You, Electrophoresis 32 (2011) 2139.
[19] G. D Christian, and W. C. Purdy, J. Electroanal. Chem. 3 (1962) 363.
[20] M. D. Meti, J. C. Abbar, S. T., Nandibewoor, and S. A. Chimatadar, Cogent Chem. 2 (2016) 1235459.
[21] E. J. J. Laviron, J. Electroanal. Chem. Inter. Electrochem. 101 (1979) 19.
[22] J. C. Abbar, M. D. Meti, and S. T. Nandibewoor, Surfaces and Interfaces 19 (2020) 100484.
[23] A. J. Bard, and L. R. Faulkner, Electrochemical Methods, Fundamentals and Applications. P (2004) 286.
[24] H. Wang, D. Qian, X. Xiao, C. Deng, L. Liao, J. Deng, and Y. W. Lin, Bioelectrochemistry 121 (2018) 115 .